Analysis of Coupled Flutter of Parallel Plates in Axial Flow by Using Monolithic Finite Element Method

Chunyu Zhang, Biao Wang*
Sino-French Institute of Nuclear Engineering & Technology,
Sun Yat-Sen University, Zhuhai, Guangdong, P. R. China, 519082

ABSTRACT
In the present paper, we use a monolithic finite element method to simulate the flutter behavior of two, three and four parallel plates experimentally studied by Schouveiler and Eloy (Phys. Fluids 21, 081703(2009)). Different coupled fluttering modes of the parallel plates are successfully reproduced. Although the results are preliminary, the essential physics of this strongly coupled system are successfully captured. No artificial constraints (i.e., the virtual spring connections between the plates) are needed to predict the in-phase mode of flutter. To the authors' best knowledge, this is the first time that one can capture all the coupled modes of flutter of multiple plates through direct numerical simulations.

Keywords: Fluid-structure interaction; finite element method; coupled flutter;

1. INTRODUCTION

As a central topic in the general subject of fluid-structure interaction, the dynamics of flexible structures (e.g. plates and shells, pipes, filaments, cylindrical tubes) in axial flow has been the main focus of a large amount of studies, motivated by applications in aerospace and nuclear engineering [1,2], aeronautics[3], civil engineering [4], biomechanics[5-7], paper industry[8], energy-harvesting [9] and many other engineering areas. As canonical examples, the instabilities of a solitary slender cylinder, a thin plate or a single filament immersed in axial flow have been thoroughly investigated through experimental observations [9-13], theoretical derivations [12-15] and numerical simulations [16-18]. With the interaction of the above mentioned simple structures with axial flows being classified as a solved issue [19] and the exhaustive results well documented by Païdoussis [20], the frontier of the topic has been advanced to investigating the dynamic behavior of more complex systems containing arrays of flexible structures such as cylindrical tube bundles and rectangular parallel-plate assemblies in nuclear reactors or heat exchangers [21].

The most notable feature of the dynamic behavior of arrays of flexible structures interacting with axial flows is the coupling between the motions of the structural elements. As one element oscillates, the pressure field around all the others is modified and unbalanced, and hence other elements are induced to oscillate in complex but definite modes [20].For example, experiments with two flexible filaments in a flowing soap film have been conducted to model the coupling between one-dimensional plate flutters [11].When placed

*Correspondence author.
Email: aracn@163.com Tel: 0756-3668967

in proximity, the two filaments were observed to flap first in phase and then out of phase with increasing the inter-plate distance. When placed at a much larger distance, flutters of both the filaments became independent. The coupling modes between the two flapping filaments were successfully simulated by using the immersed boundary method [22] and by using the Arbitrary–Lagrangian–Eulerian (ALE) finite element method [23]. A theoretical investigation also confirms the coupling modes of two cantilevered flexible plates but virtual spring connections were assumed when calculating the in-phase mode [24].

In a recent study, the coupled flutter of an assembly of two, three, and four flexible parallel cantilevered plates in a uniform axial flow were captured by a high-speed camera [25]. Depending on the flow velocity, on the inter-plate distance, and on the plate length, different coupled modes were observed. A linear analysis based on the analytical derivation due to Jia et al. [26] can capture the main characteristic of the instability of the system. However, the linear analysis fails to predict the linearly unstable modes and also fails to predict the transition from one mode to another because the analytical derivation is based on a perturbation theory [25]. Due to the inherent complexity, it is anticipated to be an even challenging task to theoretically analyze the flutter behavior of practical assemblies which usually contain tens or hundreds of structural elements immersed in complex fluids.

The successful analysis of the dynamics of a single slender structure [16-18,27] and two coupling filaments [22,23] manifests the great advantages of numerical simulations on investigating such complex problems. Motivated by these works, the major purpose of the present study is to develop an efficient and robust computational framework to study the dynamic behavior of assemblies of flexible structures in axial or more general flows. The governing equations of the flows, the solid structures as well as the fluid-structure interaction are solved as a whole by using a monolithic finite element procedure proposed by Heil et al.[27]. Then the coupled modes of two, three and four parallel plates in a uniform axial flow are calculated and compared with the experimental observations presented in Ref.[25] for the purpose of verification. It should be mentioned that the current research has not only originated from theoretical curiosity but also is related to develop a computational tool to evaluate the design of core elements of nuclear reactors.

2 MATHEMATICAL FORMULATION AND NUMERICAL METHOD

2.1 GOVERNING EQUATIONS

Assuming that all lengths and coordinates are non-dimensionalized on a problem-specific length scale L, while time is non-dimensionalized on some reference timescale T, and the fluid velocities are non-dimensionalized on a representative velocity U, the dimensionless Navier-Stokes equations, which govern the flow of an incompressible Newtonian fluid with density ρ_f and viscosity μ, are given by,

$$\begin{cases} Re\left(St\dfrac{\partial u_i}{\partial t}+u_j\dfrac{\partial u_i}{\partial x_j}\right)=-\dfrac{\partial p}{\partial x_i}+\dfrac{\partial}{\partial x_j}\left(\dfrac{\partial u_i}{\partial x_j}+\dfrac{\partial u_j}{\partial x_i}\right) \\ \dfrac{\partial u_j}{\partial x_j}=0 \end{cases} \tag{1}$$

where $Re = \rho_f UL/\mu$ is the Reynolds number, $St = L/(UT)$ is the Strouhal number, and the pressure p is non-dimensionalised on the viscous scale $\mu U/L$. Implemented in the ALE from, Eq.(1) serves as the basic governing equation of fluids in the present study.

Based on the variational principle, the governing equation for elastic solids can be written

in an integral form as [27],

$$\int \sigma^{ij}\,\delta\gamma_{ij}\,dv = \int \left(\mathbf{b} - \Lambda^2 \frac{\partial^2 \mathbf{R}_s}{\partial t^2} \right) . \delta \mathbf{R}_s dv + \oint \mathbf{f}\,\mathbf{R}_s dA \tag{2}$$

where the two integrals are performed over the undeformed reference volume and over the deformed surface of the body, respectively. The second Piola-Kirchhoff stress tensor σ^{ij}, is determined by as a function of the Green strain tensor γ_{ij} through a user-provided constitutive relationship. The stress tensor σ^{ij}, the body force **b** and the surface traction **f** are all non-dimensionalized on some characteristic stiffness parameter, S, such as Young's modulus E. Now the timescale ratio is given by where $\Lambda = (L/T)\sqrt{\rho_s / S}$ is the density of the solid. $\boldsymbol{R}_s$ is the normalized position vector and therefore, $\partial^2 \mathbf{R}_s / \partial t^2$ is the acceleration of the solid.

The changes in the domain geometry of fluids are induced by the displacements of structures through the no-slip condition,

$$\mathbf{u} = St \frac{\partial \mathbf{R}_s}{\partial t} \text{ on fluid-structure interfaces} \tag{3}$$

The traction that the Newtonian fluid exerts onto the solid is given by,

$$f_i^{[FSI]} = Q \left(-p\delta_{ij} + \left(\frac{\partial u_i}{\partial x_j} + \frac{\partial u_j}{\partial x_i} \right) \right) N_j \tag{4}$$

where the N_j are the Cartesian components of the outer unit normal on the deformed solid pointing into the fluid and the FSI parameter $Q = \mu U/(SL)$ is the ratio of the stress scales used in the non-dimensionalisation of the solid and fluid equations. The parameter Q indicates the strength of the fluid-structure interaction in that as Q tends to zero, the fluid stresses exerted onto the structures become negligible.

2.2 NUMERICAL PROCEDURE

The above governing equations can be solved by various numerical techniques (e.g. finite element method or control volume method) either separately or as a whole. In the separated (segregated) approach, the fluid problem and the solid problem are alternatively solved and then coupled via fixed point (Picard) iteration. While in the monolithic approach, the complete system of nonlinear algebraic equations that arises from the coupled discretisation of the equations of motion in the fluid and solid domains is solved as a whole, typically using a variant of Newton's method. Although the segregated approach can treat the separate fluid and solid solvers as "black-boxes" and therefore can take advantage of existing commercial codes as demonstrated in Ref.[18], its low efficiency and poor convergence performance for strongly coupling problems preclude the method from our present research and the monolithic approach is preferably chosen for its robustness and efficiency.

In the present research, an object-oriented FSI solver adopting monolithic discretisation is developed on top of the multi-physics finite element library OOMPH-LIB [27]. To ensure a good modularity and a concise program structure, C++ inheritance and template programming are routinely used. Interfaces to mesh data generated by third-party meshing tools are developed and therefore, 'arbitrary' fluid and solid domains can be defined by providing mesh data files. The fluid inlet and the outlet boundaries as well as the fluid-structure interfaces can be conveniently defined by specifying the node sets defined in the mesh data files. Taylor-Hood (Q2Q1) elements are adopted to assemble the fluid domain and conventional Galerkin elements for the solid domain. Mesh deformation in response to wall deformation is achieved through an algebraic node update strategy and unlike the method

used in Ref.[16], no shared nodes are required on the fluid-structure interfaces in the present method.

3 NUMERICAL SIMULATIONS AND RESULTS

3.1 MODEL SETUP

According to Schouveiler and Eloy's experiments [25], the plate assembly was confined between two horizontal plates in order to limit three-dimensional effects. Therefore, the experimental setup can be approximately described by a two-dimensional model (Fig.1). The experiment parameters and the simulation parameters are listed in Table I. In the numerical model, the domain size is truncated and the thickness of the plate is increased (while the flexural rigidity is maintained) in order to control the computation cost by limiting the total number of finite elements. The spatial convergence of the present finite element mesh with an average length of 0.5mm has already been checked by making a comparison with a one and a half times fine-divided mesh. Good agreements between the present mesh and the finer mesh solutions of both the flapping frequency and amplitude are obtained. The relative differences are within the order of 1%.

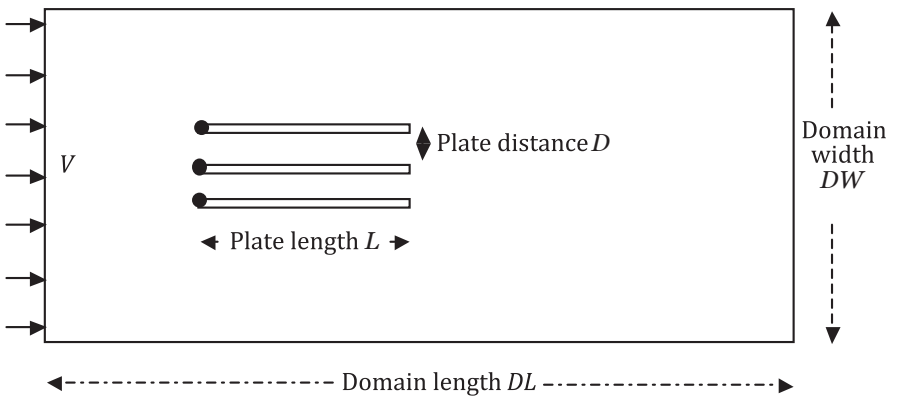

Figure 1. Sketch of the experimental setup by Schouveiler et al. [25]

Table I. Parameters of laboratory experiment [25] and present numerical simulations

Parameters	Experimental values	Simulation values
Domain length, *DL*	---	75cm
Domain width, *DW*	80cm	25cm
Plate length, *L*	10~25cm	18cm
Plate thickness	0.28mm	6.0mm
Number of plates	2,3,4	2,3,4
Plate distance, *D*	1.0~17.0cm	0.6~6.0cm
Air dynamic viscosity	1.817×10^{-5}Pa-s	1.817×10^{-5}Pa-s
Air density	1.2 Kg/m^3	1.2 Kg/m^3
Air inflow velocity, *V*	5.0~30.0m/s	5.0~30.0m/s
Plate flexural rigidity, *G*	9.7×10^{-3}N.m	3.2×10^{-3}N.m
Plate density	1571.4Kg/m^3	1571.4Kg/m^3
Gravitational acceleration	9.8m/s^2	9.8m/s^2

In the present simulations, the inflow velocity is ramped up to the specified level within 1*s* and then fixed throughout the calculations. The outflow condition of the domain is assumed to be traction free. The plates are cantilevered by their upwinding ends (indicated by the solid circles in Fig.1) and a gravity force in the flow direction is applied to the plates. Both the domain geometries and the finite element meshes are generated by an open-source pre/post-processing software, i.e. Salome [28] and all the boundaries are defined as node sets.

3.2 SIMULATED COUPLED FLUTTER OF PARALLEL PLATES IN AXIAL FLOW

Typical snapshots of the simulated flutter behavior of two, three and four parallel plates are respectively shown in Fig.2, Fig.3 and Fig.4. Consistent with experimental observations, different coupling modes of flutter can be identified.

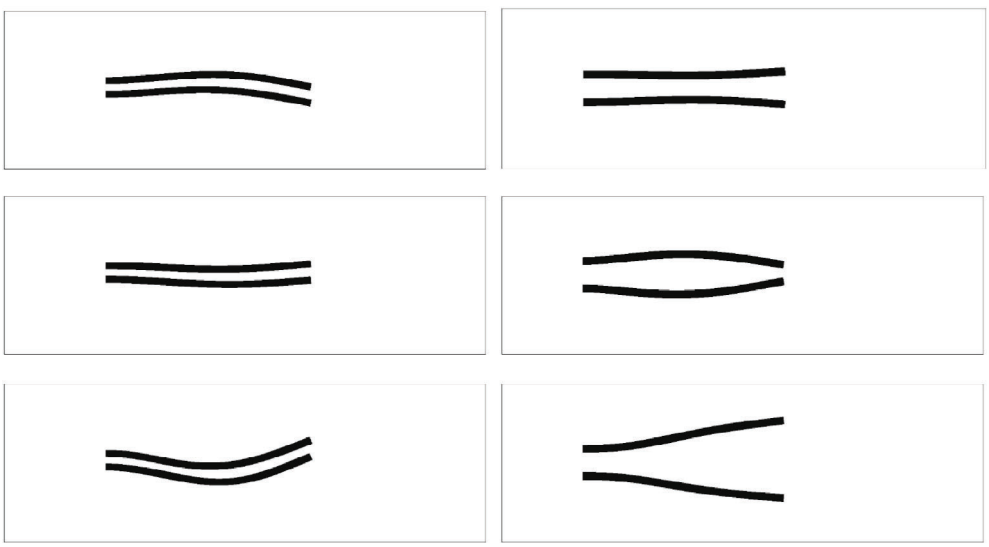

Figure 2. Typical snapshots of (a) in-phase flutter with D=0.6cm and (b) anti-phase flutter with D=1.8cm of two parallel plates. For both type of coupled flutter, the air inflow velocity V=9.0m/s.

For the two-plate system, experimental measurements [25] ascertain that both the two possible coupled flutter share the same vibration amplitude as manifested in Fig.2. However, for the three-plate system (Fig.3) and the four-plate system (Fig.4), both experiments and simulations show that the flutter amplitude of the inner plates is higher that of the outer plates except Mode (b) of the three-plate system in which the middle plate does not flutter.

Both the experiments [25] and the present simulations show that the plates may touch each other if the inflow velocity is high enough (Fig.5. Once the plates get touched, the simulations terminate due to severe distortion of the fluid mesh). However, it is declared that the structures can never touch each other due to the pressure forces in the intervening fluid [23]. The possible reason is that the structure in [23] is stiffer than the present structure.

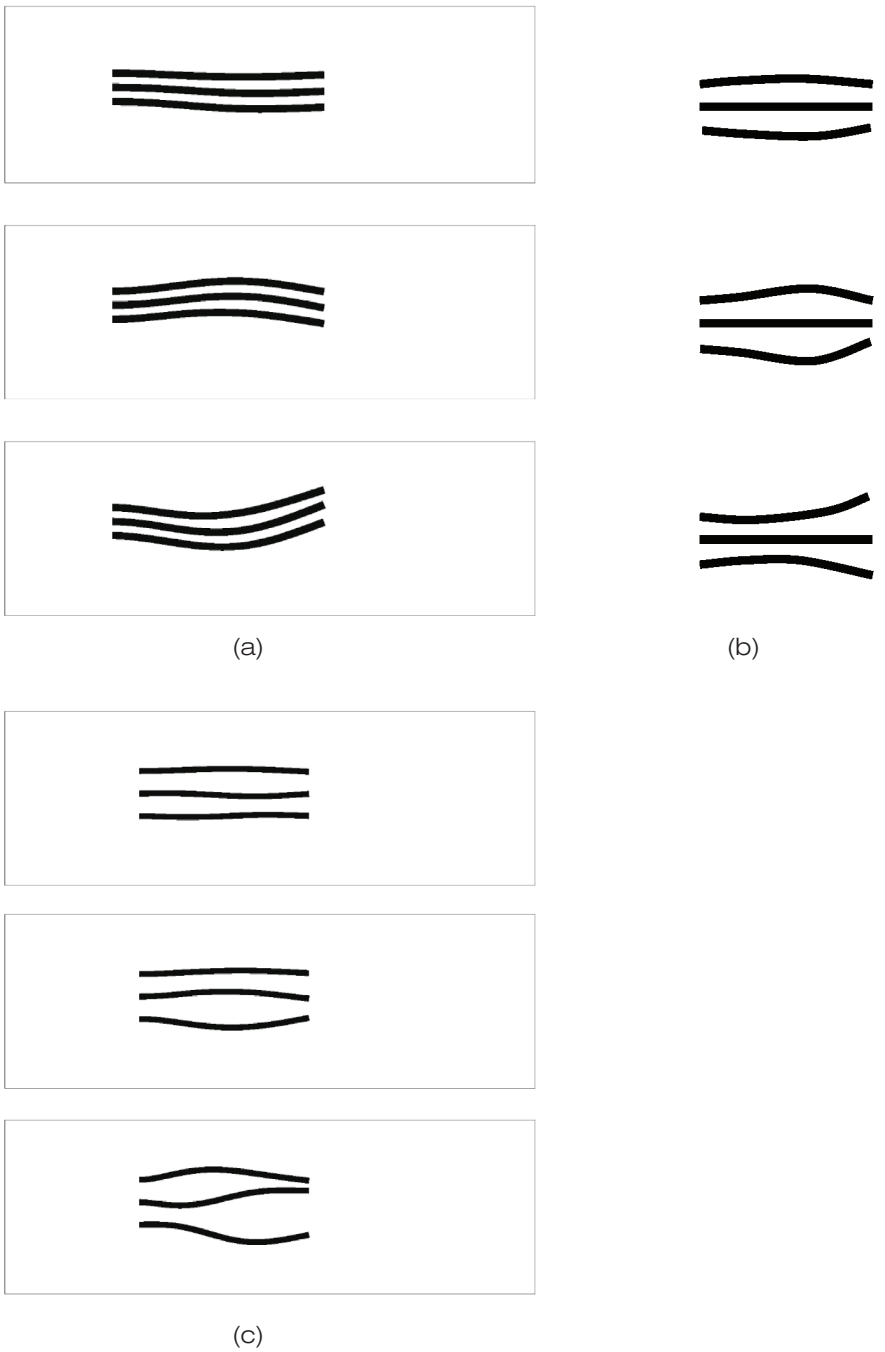

Figure 3. Typical snapshots of (a) in-phase flutter with D=0.6cm and V=11.0m/s (b) anti-phase flutter with D=1.8cm and V=7.0m/s, and (c) hybrid flutter with D=1.8cm, V=14.0m/s of three parallel plates.

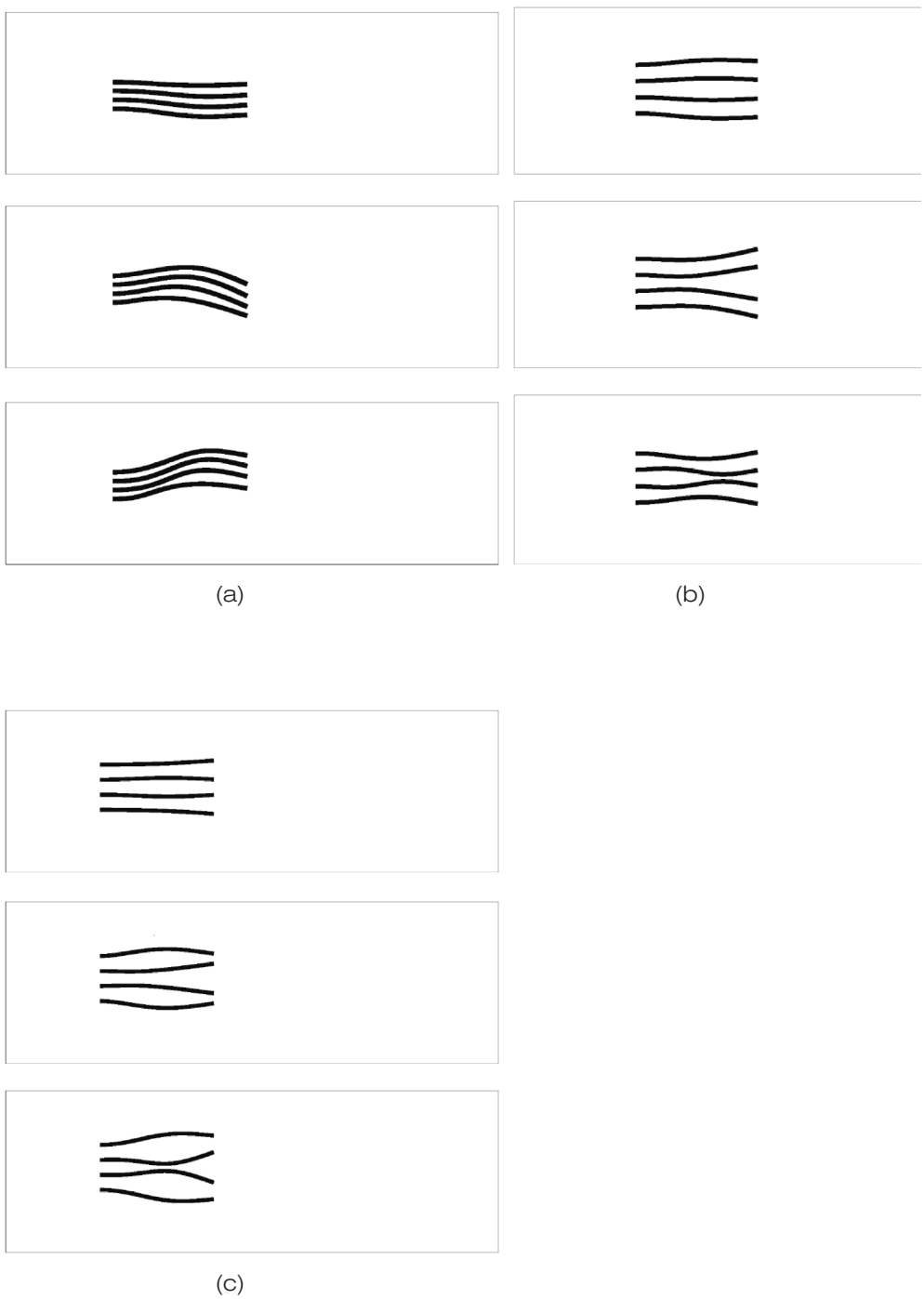

Figure 4. Typical snapshots of (a) in-phase flutter with D=0.6cm and V=11.0m/s (b) anti-phase flutter with D=1.8cm and V=15.0m/s, and (c) hybrid flutter with D=2.0cm and V=10.0m/s of four parallel plates.

Figure 5. Touch of plates due to high inflow velocity.

Typical pressure fields of the two-plate, the three-plate and the four-plate systems are shown in Fig.6, Fig.7 and Fig.8, respectively. In all the figures, the red region denotes high pressure and the blue region denotes low pressure. It is evident that if the in-phase flutter (Fig.6(a), Fig.7(a) and Fig.8(a)) occurs, the low-pressure region is located at the outermost side while if the anti-phase or the hybrid flutter occur, the low-pressure region is located in between the plates.

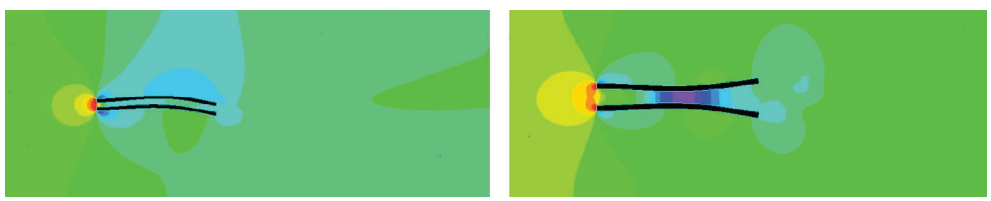

(a) (b)

Figure 6. Typical contours of the pressure field of (a) in-phase flutter and (b) anti-phase flutter in the two-plate system.

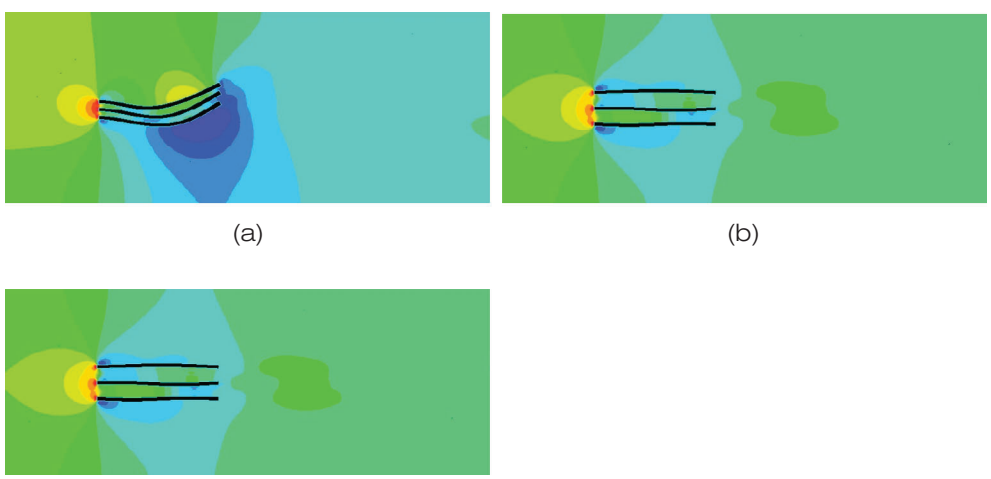

(a) (b)

(c)

Figure 7. Typical contours of the pressure field of (a) in-phase flutter, (b) anti-phase flutter, and (c) hybrid flutter in the three-plate system.

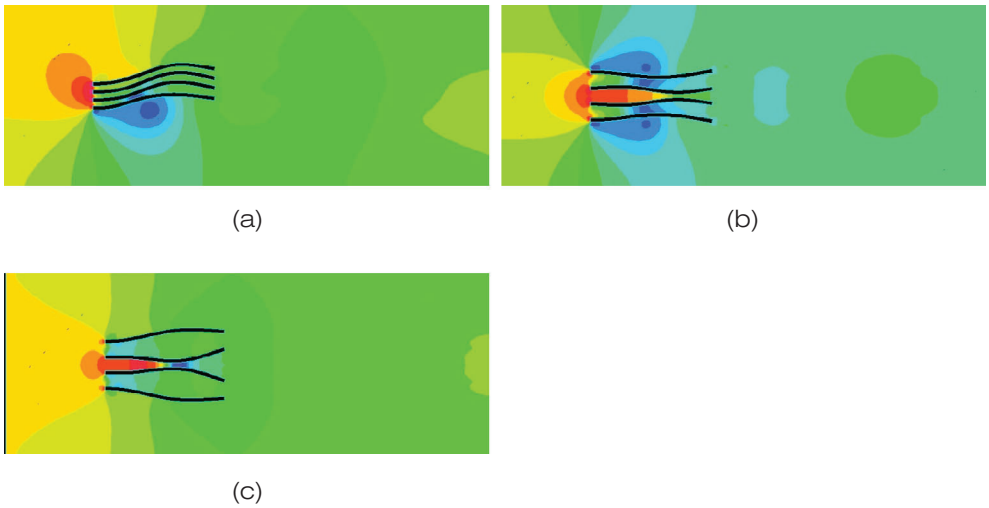

Figure 8. Typical contours of the pressure field of (a) in-phase flutter, (b) anti-phase flutter, and (c) hybrid flutter in the four-plate system.

3.3 EFFECTS OF THE INTRINSIC FSI PARAMETERS

Although complex, the coupled modes of flutter can be completely determined by solving the governing equations, i.e. Eqs.(1)-(4). A specific mode of flutter depends only on the intrinsic parameters, e.g., the Reynolds number, the Strouhal number, the FSI parameter Q and the timescale Λ. Through varying these important parameters, different coupled mode of flutter can be achieved. For example, by reducing the timescale, i.e. Λ, through decreasing the density of structure, the flutter can be effectively suppressed. For a massless or sufficiently small mass structure, no flutter can be excited or sustained [11,16,17]. This is easily understood by checking the governing equation of the solids, i.e., Eq.(2). When the density of the solid approaches to zero, the intrinsic timescale of the solid, i.e. Λ, also approaches to zero and the governing equation of dynamics reduces to a steady equation.

The effect of the Reynolds number on the flutter mode has been investigated by Schouveiler and Eloy through parametric experimental studies [25]. Compared with the Reynolds number, the FSI parameter, i.e. Q, is more easily tuned through engineering measures, for example, by changing the rigidity of the flexible structure. Our simulations show that by solely changing plate flexural rigidity, different coupled modes of flutter can also be achieved.

4. SUMMARY AND CONCLUSIONS

In the present paper, we employ an in-house developed FSI solver to simulate the flutter behavior of two, three and four parallel plates experimentally studied by Schouveiler and Eloy [25]. A monolithic finite element method is applied to solve the governing equations of the fluid, the structures and the fluid-structure interactions. Different coupled fluttering modes of parallel plates are successfully reproduced. Although the results are clearly preliminary, the essential physics of this strongly coupled system are still successfully captured. Unlike the method due to Tang et al.[24], no artificial constraints (i.e., the virtual spring connections between the plates) are needed to predict the in-phase mode of flutter. To the authors' best knowledge, this is the first time that one can capture all the coupled modes of flutter of

multiple plates through direct numerical simulations. In addition, it has been shown that the ALE finite element method introduces less artificial damping than the immersed boundary method [16]. So we believe that after necessary extensions (e.g., incorporation of turbulence modeling), the present numerical procedure would be a promising tool to quantitatively investigate the effects of engineering parameters (e.g., rigidity of structural elements, space between the structural elements, applied external constraints exerted, inflow velocity) on the coupled dynamic behavior of arrays of slender structures.

ACKNOWLEDGEMENT

Financial support from the National Natural Science Foundation of China (Grant No. 11002057) is gratefully acknowledged.

REFERENCES

[1] Dowell EH. *Aeroelasticity of Plates and Shells*, 1st[ed]. Noordhoff International Publishing, Leyden, 1975.

[2] Chen SS. Vibration of nuclear fuel bundles. *Nucl Eng Des* 1975; 35:399–422.

[3] Kornecki A, Dowell EH, O'Brien J. On the aeroelastic instability of two-dimensional panels in uniform incompressible flow. *J Sound Vib* 1976;47:163–178.

[4] Housner GW. Bending vibrations of a pipeline containing flowing fluid. *J Appl Mech* 1952;19: 205-208.

[5] Taylor G. Analysis of the swimming of long and narrow animals. *Proc Roy Soc Lond A – Math Phys Sci* 1952; 214:158–83.

[6] Huang L. Flutter of cantilevered plates in axial flow. *J Fluids Struct* 1995; 9:127–147.

[7] Huber G. Swimming in Flatsea, *Nature* 2000; 48:777-778.

[8] Watanabe Y, Suzuki S, Sugihara M, Sueoka Y. An experimental study of paper flutter. *J Fluids Struct* 2002;16: 529–542.

[9] Tang L., The dynamics of two-dimensional cantilevered flexible plates in axial flow and a new energy-harvesting concept, PhD Thesis, McGill University, Montréal, Québec, November 2007.

[10] Païdoussis MP, Dynamics of flexible slender cylinders in axial flow. Part 2. Experiments. *J Fluid Mech* 1966; 2:737-751.

[11] Zhang J, Childress S, Libchaber A, Shelley M. Flexible filaments in a flowing soap film as a model for one-dimensional flags in a two-dimensional wind. *Nature* 2000; 408:835–839.

[12] Tang DM, Yamamoto H, Dowell EH. Flutter and limit cycle oscillations of two-dimensional panels in three-dimensional axial flow. *J Fluids Struct* 2003; 17: 225–242.

[13] Zhao WS, Païdoussis MP, Tang LS, Liu MQ, Jiang J. Theoretical and experimental investigations of the dynamics of cantilevered flexible plates subjected to axial flow. *J Sound Vib* 2012; 331:575–587.

[14] Païdoussis MP. Dynamics of flexible slender cylinders in axial flow. Part 1. Theory. *J Fluid Mech* 1966; 26:717-736.

[15] Tang L, Païdoussis MP. On the instability and the post-critical behavior of two-dimensional cantilevered flexible plates in axial flow, *J Sound Vib* 2007; 305:97–115.

[16] Sawada T, Hisada T. Fluid–structure interaction analysis of the two-dimensional flag-in-wind problem by an interface-tracking ALE finite element method. *Comput Fluids* 2007;36:136–146.

[17] Zhu L, Peskin CS, Simulation of a flapping flexible filament in a flowing soap film by the immersed boundary method. *Comput Phys* 2002; 179:452–68.

[18] Liu ZG, Liu Y, Lu J. Fluid–structure interaction of single flexible cylinder in axial flow. *Comput Fluids* 2012; 56:143–151.

[19] Païdoussis MP. Some unresolved issues in fluid-structure interactions. *J Fluids Struct* 2005; 20: 871–890.

[20] Païdoussis, MP. *Fluid–structure interactions slender structures and axial flow*. vol.2. Elsevier, Academic Press, London,1998.

[21] Guo CQ, Païdoussis MP. Analysis of hydroelastic instabilities of rectangular parallel-plate assemblies. *J Press Vess-T* ASME 2000;122:502–508.

[22] Zhu LD, Peskin CS. Interaction of two flapping filaments in a flowing soap film. *Phys Fluids* 2003;15:1954-1960.

[23] Farnell DJJ, David T, Barton DC. Coupled states of flapping flags. *J Fluids Struct* 2004; 19:29–36.

[24] Tang L, Païdoussis MP. The coupled dynamics of two cantilevered flexible plates in axial flow. *J Sound Vib* 2009; 323:790–801.

[25] Schouveiler L, Eloy C. Coupled flutter of parallel plates. *Phys Fluids* 2009; 21: 081703.

[26] Jia LB, Li F, Yin XZ, Yin XY. Coupling modes between two flapping filaments. *J Fluid Mech* 2007; 581:199-220.

[27] Heil M, Hazel AL. oomph-lib—An object-oriented multi-physics finite-element library. In: Schafer M, Bungartz H-J(eds) *Fluid–structure interaction*. Springer 2006; 19–49.

[28] Salome, The open source integration platform for numerical simulation, http://www.salome-platform.org/